GEOPHYSICS, VOL. 53, NO. 5 (MAY 1988); P. 707 720, 13 FIGS., 3 TABLES.

Inversion of bottom-hole temperature data: The Pineview field, Utah-Wyoming thrust belt

Dave Deming* and David S. Chapman‡

ABSTRACT

The present day temperature field in a sedimentary basin is a constraint on the maturation of hydrocarbons; this temperature field may be estimated by inverting corrected bottom-hole temperature (BHT) data. Thirty-two BHTs from the Pineview oil field are corrected for drilling disturbances by a Horner plot and inverted for the geothermal gradient in nine formations. Both least-squares (ℓ_2) norm and uniform (ℓ_1) norm inversions are used; the ℓ_1 norm is found to be more robust for the Pineview data. The inversion removes random error from the corrected BHT data by partitioning scatter between noise associated with the BHT measurement and correction processes and local variations in the geothermal gradient. Three-hundred thermal-conductivity and density measurements on drill cuttings are used, together with formation density logs, to estimate the in situ thermal conductivity of six of the nine formations. The thermal-conductivity estimates are used in a finite-element model to evaluate 2-D conductive heat refraction and, for a series of inversions of synthetic data, to assess the influence of systematic and random noise on the inversion results. A temperature-anomaly map illustrates that a temperature field calculated by a forward application of the inversion results has less error than any single corrected BHT. Mean background heat flow at Pineview is found to be 61 mW/m^2 (± 13 percent), but is locally higher (65 mW/m^2) due to heat refraction. The BHT inversion (1) is limited by systematic noise or model error, (2) achieves excellent resolution of a temperature field although resolution of individual formation gradients may be poor, and (3) generally cannot detect lateral variations in heat flow unless thermal-conductivity structure is constrained.

INTRODUCTION

The temperature history of a sedimentary basin determines the maturation of kerogen into petroleum and the conversion of oil into gas. A critical constraint on any temperature history that is used to calculate maturation indices by schemes such as Lopatin's method (Waples, 1980) is the present day thermal state. Indeed, the most common assumption in maturation studies is that the present day thermal state has remained constant through time (Leadholm et al., 1985; Edman and Surdam, 1984).

The thermal analysis of a sedimentary basin is hampered, however, by lack of high-quality temperature data. High-precision measurement of in situ temperatures is generally limited to a few relatively shallow boreholes that have been drilled for mineral or water exploration, for example. For most basins, though, numerous bottom-hole temperatures (BHTs), temperatures measured at the bottom of a well during geophysical logging, are available. Several tens of thousands of BHTs are available for the thermal analysis of individual basins or fields; the AAPG data file (Am. Assn. Petr. Geol., 1976) contains more than 28 000 BHT entries for North America.

Unfortunately, the quality of the BHT data is low. Due to a transient drilling disturbance, BHTs are generally lower than true equilibrium temperatures by up to 15 percent (Jam et al., 1969). The scatter around any mean error is large, and an individual temperature measurement may be in error by as much as 20 C. Although a correction is usually applied in an attempt to obtain a zero-mean error for the entire data set, evaluating the nature of the remaining random error is problematical; individual corrected BHTs may be spurious. Figure 1, which shows corrected BHTs from the Pineview field, illustrates a typical BHT-depth distribution. At a depth of 3 km

Manuscript received by the Editor February 3, 1987; revised manuscript received September 29, 1987.
*Department of Geology and Geophysics, University of Utah, Salt Lake City, UT 84112.
‡Department of Geology and Geophysics, University of Utah, and Pacific Geoscience Center, Geological Survey of Canada, Sidney, B.C., Canada V8L 4B2.

the scatter in the temperature data is about ±5°C, but the difference between individual BHTs is as great as 35°C. The fundamental problem in interpreting these data is that it is not clear how much of the scatter is due to random noise associated with the BHT measurement and correction processes and how much reflects geologic signal, namely, local changes in the geothermal gradient.

Numerous recent studies of basins have used BHTs for different types of thermal analyses (see, for example, Majorowicz and Jessop, 1981; Chapman et al., 1984; Andrews-Speed et al., 1984; Speece et al., 1985; Reiter et al., 1986; and Willett and Chapman, 1987), but there is little uniformity in methods used to process BHT data. Most investigators recognize the inherent noise in BHT data, but there has been no consensus on evaluating the consequences of this noise. As part of a broad program to analyze and interpret the thermal state of sedimentary basins, we have been seeking optimum methods for analyzing the large amount of BHT data available. In this paper we describe a detailed study of one spatially restricted, but otherwise typical, BHT data set. We apply an inversion methodology, first used by Speece et al. (1985) in the Michigan Basin, to BHT data (Figure 1) from the Pineview oil field in the Utah-Wyoming thrust belt, a small (3 km × 5 km) structurally complex area. We address the problem of recognizing the distribution and magnitude of noise in the BHT data, in particular the problem of recognizing individual BHTs that have large (>20°C) errors. We also introduce the concept of temperature-anomaly maps and use them to evaluate different thermal models. Finally, the strengths and shortcomings of the inversion methodology are examined in a series of synthetic inversions that critically assess the influence of error in the BHT data on the inversion results.

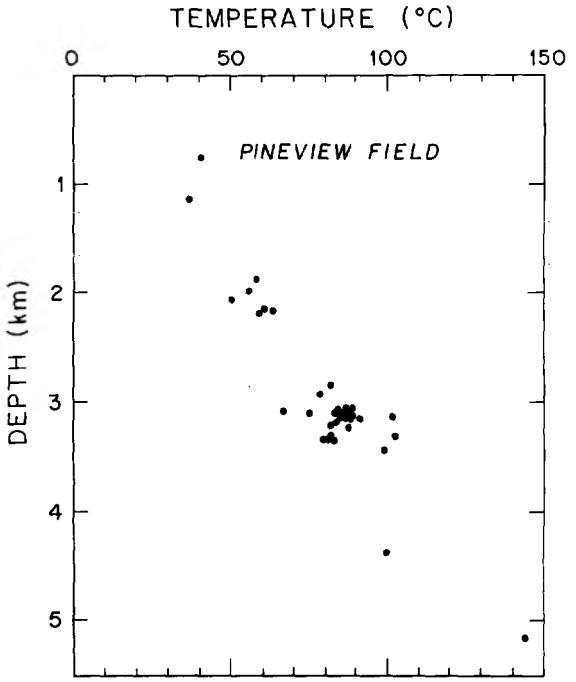

FIG. 1. Bottom-hole temperatures (BHTs) from the Pineview oil field to which Horner corrections have been applied. The temperature spread at 3 km is as great as 35°C. A least-squares fit to the BHTs and corresponding mean annual surface temperatures yields an average gradient of 24°C/km.

THE PINEVIEW FIELD

Geology

The Pineview field is located in the Utah-Wyoming thrust belt (Figure 2), an area that has been the locus of intense petroleum exploration since the original discovery at Pineview in 1975. Source rocks for Pineview oil (Warner, 1982) were deposited in the Fossil basin (Figure 2), a late Cretaceous-early Tertiary foreland basin (Lamerson, 1982). Subsequent thrusting placed lower Mesozoic rocks on top of Cretaceous sediments, destroying the original basin structure. The Absaroka thrust (Figure 3) marks the unconformity at which Jurassic petroleum-reservoir rocks overlie the Cretaceous source sediments. The study area contains a dense cluster of 43 wells within an area of 3 km × 5 km (Figure 4). For the purpose of the thermal analysis, the stratigraphy (Figure 5) was divided into nine units penetrated by a majority of the wells at Pineview. The thickness of each of these nine units at each borehole was obtained from well records which list the depth to the top of each formation.

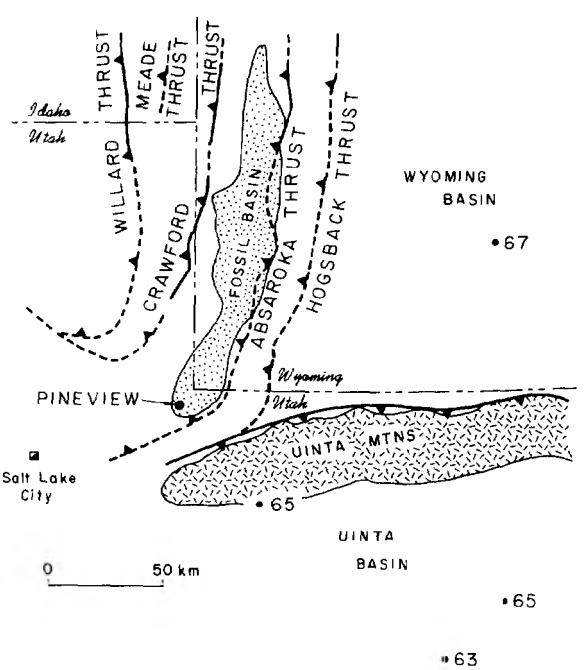

FIG. 2. The Pineview oil field is located in the southern part of the Fossil Basin as defined by Lamerson (1982); major faults of the Utah-Wyoming thrust belt are shown. Solid circles show heat-flow estimates in mW/m² from other studies (Sass et al., 1971b; Reiter et al., 1979; and Bauer and Chapman, 1986).

Temperature data

A bottom-hole temperature (BHT) is the temperature measured at the bottom of an oil or gas well during routine geophysical logging. Due to a transient disturbance associated with the circulation of drilling mud, BHTs are generally lower

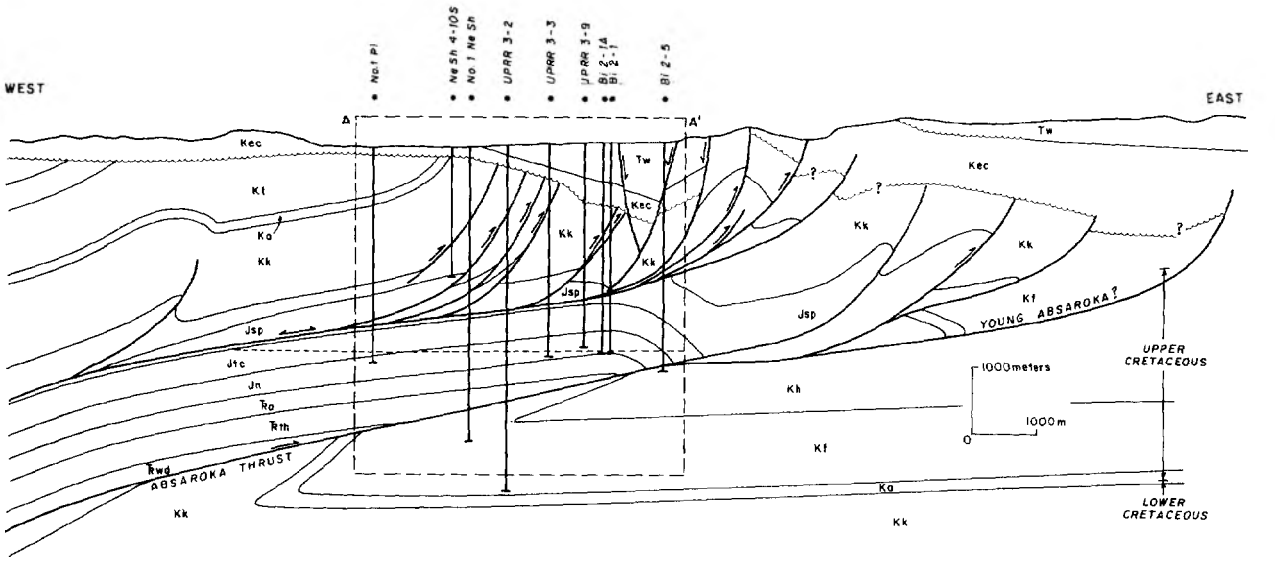

FIG. 3. Cross-section through part of the Utah-Wyoming thrust belt after Lamerson (1982). The Pineview field is located within the dashed rectangle. The dominant structural feature is the Absaroka thrust fault which has placed lower Mesozoic rocks on top of Cretaceous basin sediments. In the boxed area, the figure has been modified from Lamerson (1982) to match our interpretation of the stratigraphy at Pineview. East of the field, the use of the symbols Kec and Tw merely reflects thermal conductivities used in the finite-element model.

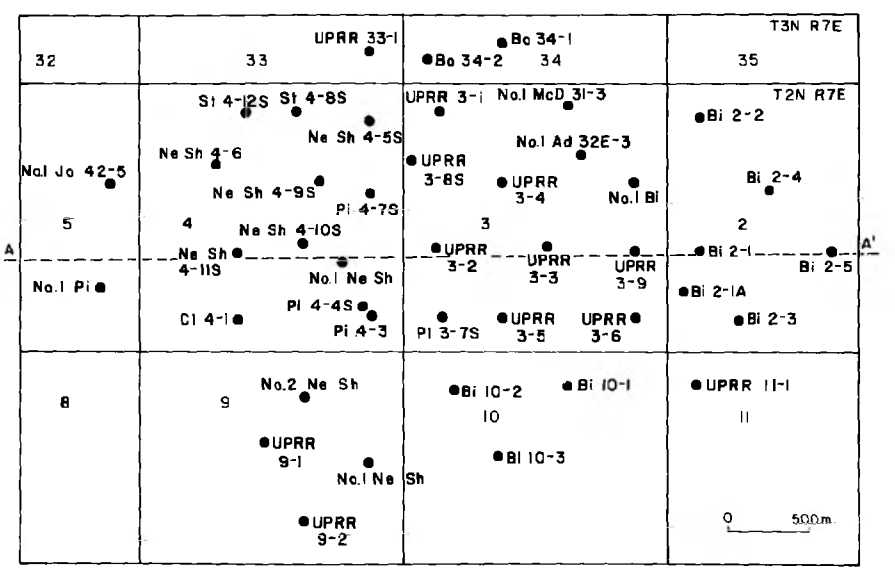

FIG. 4. The Pineview oil field (Summit County, northeast Utah) consists of a dense cluster of 43 wells in an area that is approximately 3 km × 5 km. Township, range, and section numbers are shown, together with well names. Line A-A′ corresponds to the cross-section shown in Figure 3.

than true, undisturbed formation temperatures. Thus raw BHTs collected from log headers must be corrected before they can be used in a thermal analysis. In this study we use the Horner plot correction as applied by Chapman et al. (1984). The Horner plot requires two or more temperature measurements, made at the same depth in the same well, but at different times. Each sequence of BHT measurements is used to predict an equilibrium temperature (corrected BHT) that is an estimate of the true formation temperature.

Scrutiny of original log records and *careful* screening of data are essential first steps in the analysis of BHT data. The Pineview data were gathered from microfilm copies of well logs on file at the Utah oil and gas commission. Forty-three wells at Pineview yield 32 sets of two or more temperature measurements suitable for Horner corrections and subsequent inclusion in the inversion analysis. The quality of these data is comparatively high. Successive logging runs in a borehole generally yield a sequence of BHTs consistent with the physics governing the conductive transfer of heat into a well during equilibration. Those runs that do not yield consistent results are rejected. Temperatures measured less than 4 hours after the cessation of circulation are also rejected as being unsuitable for Horner plot corrections. The Horner correction must not be applied indiscriminately: it is based on a number of simplifying assumptions concerning the nature of heat transfer into a well.

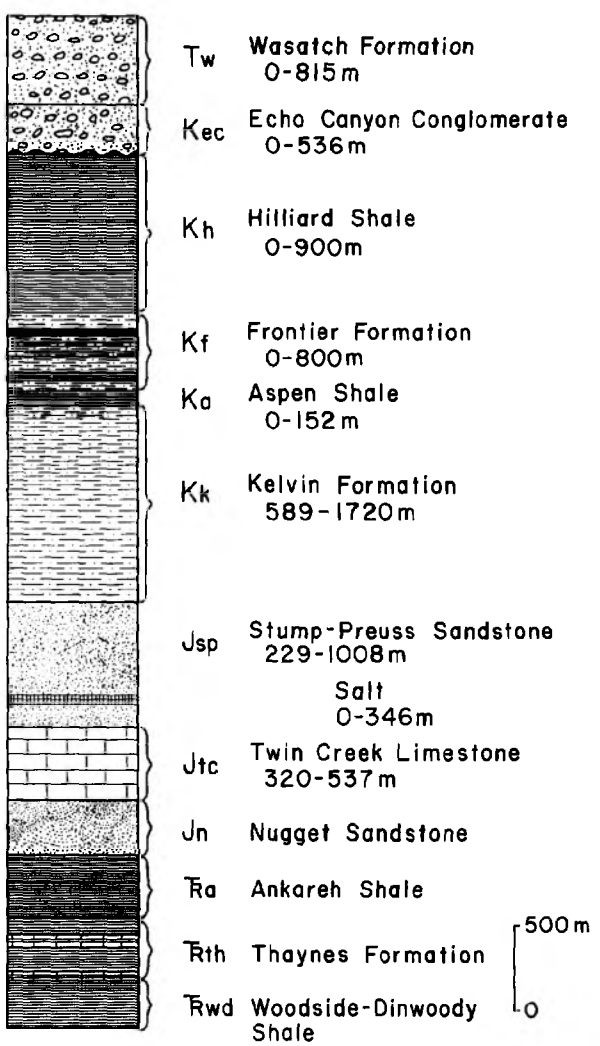

FIG. 5. Stratigraphic column for the Pineview area. All of the formations shown, from the Nugget formation up, were included in the thermal analysis, with the exception of the Hilliard shale which occurs only in the Cretaceous section below the Absaroka thrust fault.

BHT corrections and the Horner plot in particular have been discussed extensively in the literature (see, for example, Luheshi, 1983, for a recent comprehensive discussion and reference list). On the basis of these theoretical and observational considerations, we conclude that the error in equilibrium temperature estimates is unlikely to be more than 10°C. On the other hand, measurement inaccuracy and uncertainty in correction parameters imply that the error is certainly greater than 1°C. Therefore, we bracket the probable error and make an a priori estimate that the error in any one equilibrium temperature is on the order of 5°C. This is consistent with Reiter et al. (1986, p. 6231), who estimate the error in Horner-type corrections as being on the order of 3°C. However, it is possible for any single estimate to have a large (>10°C) error due to human error or other spurious factors. The temperature data set was completed by estimating mean annual surface temperatures T_0, using meteorological data and well elevations and compensating for air-ground temperature differences. The error involved in surface temperature estimations is on the order of 2°C to 3°C.

The complete temperature data set used in the inversion consists of 32 temperature differences ΔT. Each ΔT is the difference between a corrected BHT (equilibrium-temperature estimate) and an estimated surface-temperature T_0. As the error in the surface temperatures is uncorrelated with the error in the BHTs, the error in any individual ΔT is on the order of 5°C.

INVERSE THEORY

Assumptions upon which the inverse formulation is based are (1) heat transfer is one-dimensional and conductive and (2) the average geothermal gradient within a formation is constant over the lateral extent of the field. Given these assumptions, for each well we write the forward problem as

$$\Delta T_i = \sum_{j=1}^{m} z_{ij} g_j, \qquad i = 1, 2, \ldots, n, \tag{1}$$

where ΔT_i is the temperature difference at the ith well, z_{ij} is the thickness of the jth formation at the ith well, and g_j is the geothermal gradient in the jth formation. In matrix form,

$$\mathbf{T}_\Delta = \mathbf{Z}\mathbf{g}, \tag{2}$$

where $\mathbf{T}_\Delta$ is the vector of n temperature differences, $\mathbf{Z}$ is an $n \times m$ matrix of formation thicknesses, and $\mathbf{g}$ is the vector of m unknown formation gradients. For the Pineview data, the number of wells $n = 32$, and the number of formations $m = 9$.

The inversion problem is to find a vector $\mathbf{g}_{est}$ that is the best estimate of the true formation gradients according to some criterion; the optimal criterion depends upon the nature of the error in the data. If errors in the data have a zero mean and are uncorrelated with a normal distribution, then a least-squares (l_2) inversion is most likely to approximate the true

model. The l_2 formulation also returns an estimate of variance σ_d^2 in the data and variance σ_m^2 of each of the elements of the solution vector (formation thermal gradients) (Menke, 1984). However, if there are a few data points with relatively large errors, a uniform norm (l_1) inversion may give better results, since it is less sensitive to noise in the data, i.e., it is more robust.

An ordinary least-squares (OLS) solution does not preclude negative gradients. Since negative geothermal gradients are usually geologically unreasonable, the estimated gradients should be constrained to be nonnegative. To implement this constraint, we have used the algorithm NNLS (nonnegative least squares) described in Lawson and Hansen (1974, p. 160). The l_1 solution was found by posing equation (2) as a linear programming problem (Menke, 1984, p. 138), which was solved using the well-known simplex algorithm.

THERMAL FIELD SOLUTION

Formation thermal gradients

The estimated gradients from the l_1 and l_2 inversions are given in Table 1. The l_2 gradients, except for the salt, vary from 21.4°C/km to 28.3°C/km. The corresponding l_2 average gradient (inversion with only one layer) is 23.9°C/km.

Although all of the gradients are physically reasonable (with the exception of the one for salt), the initial solution should be viewed with some suspicion. Note that the l_1 initial solution is significantly different from the l_2 (NNLS) solution. For example, in the Stump-Preuss formation the l_2 estimated gradient is 21.6 C/km, while the l_1 gradient is 14.9°C/km. Also, the l_2 gradients are not consistent with thermal conductivities based on formation composition. Because geothermal gradients should be inversely proportional to thermal conductivity, we expect the Aspen shale to have one of the highest gradients and the Echo Canyon quartzite conglomerate to have one of the lowest. Instead, the situation is reversed. Also, the estimated standard deviation of the temperature data σ_d is 7.7°C, higher than our a priori expectation of 5°C.

An examination of the temperature residuals (Figure 6) is revealing: three residuals are on the order of +20°C. We tested the effect of these outlying data points on the analyses by removing the data points representing the highest residuals one at a time and repeating the analysis. The effect on the l_2 (NNLS) solution is shown in Figure 7a. As the noisy data points are removed, the stability of the solution increases. After removal of the three BHTs with +20°C residuals, the estimated standard deviation of the temperature data is 5°C; and the l_2 solution has stabilized to values similar to those of the l_1 solution. We choose the preferred solution (Table 1) as that found when the three points have been removed. The l_1 solution (Figure 7b), on the other hand, remains essentially unchanged by this process, confirming that it is in fact more robust for these data.

With the exception of the Kelvin formation, all of the estimated gradients from the l_2 solution have large standard deviations σ_m (Table 1) that are correlated with the thickness of the formation in the matrix $\mathbf{Z}$. A similar correlation was found by Speece et al. (1985) in their analysis of BHT data from the Michigan Basin. This correlation simply means that formations that are poorly represented in $\mathbf{Z}$ can tolerate a large uncertainty in their estimated gradients without affecting the total temperature field significantly. A different type of algorithm could have been used to constrain the gradient in the salt to a lower limit, of say 10°C/km, but given the very poor representation of the salt in the matrix of total thicknesses (1.6 percent), it is unlikely that changing algorithms would have made a significant difference.

The temperature field

The estimated gradients g_{est_j} can be used to calculate a temperature field

$$T_{\mathrm{est}} = T_0 + \sum_j g_{\mathrm{est}_j} z_j$$

that is the best estimate of the actual temperature field at Pineview. Figure 8 shows T_{est}, constructed using the preferred l_2 gradients (Table 1), superimposed on the east-west structural cross-section shown previously in Figure 3. For comparison, eight corrected BHTs (equilibrium-temperature estimates) are shown. It is important to recognize that the accuracy of the estimated temperature field is not judged by a comparison with this subset of the corrected BHT data, since the corrected

Table 1. Formation thermal gradients determined from inversion of BHT data.

Formation	Drilled Thickness (%)	Initial solution gradients (°C/km)		Preferred solution gradients (°C/km)		
		l_2	l_1	l_2	l_1	σ_m
Wasatch	14.7	24.8	22.2	18.6	22.2	7.8
Echo Canyon	5.3	28.3	20.5	17.2	20.1	10.6
Frontier	4.7	26.5	22.8	22.2	22.9	7.4
Aspen	1.9	21.4	30.0	44.1	30.5	32.2
Kelvin	37.0	25.7	27.5	26.4	27.5	2.9
Stump-Preuss	20.3	21.6	14.9	13.5	14.8	7.3
Salt	1.6	0.0	0.0	0.0	0.0	63.1
Twin Creek	10.7	26.4	39.2	42.5	39.1	13.6
Nugget	3.8	27.5	22.4	38.6	22.8	12.1

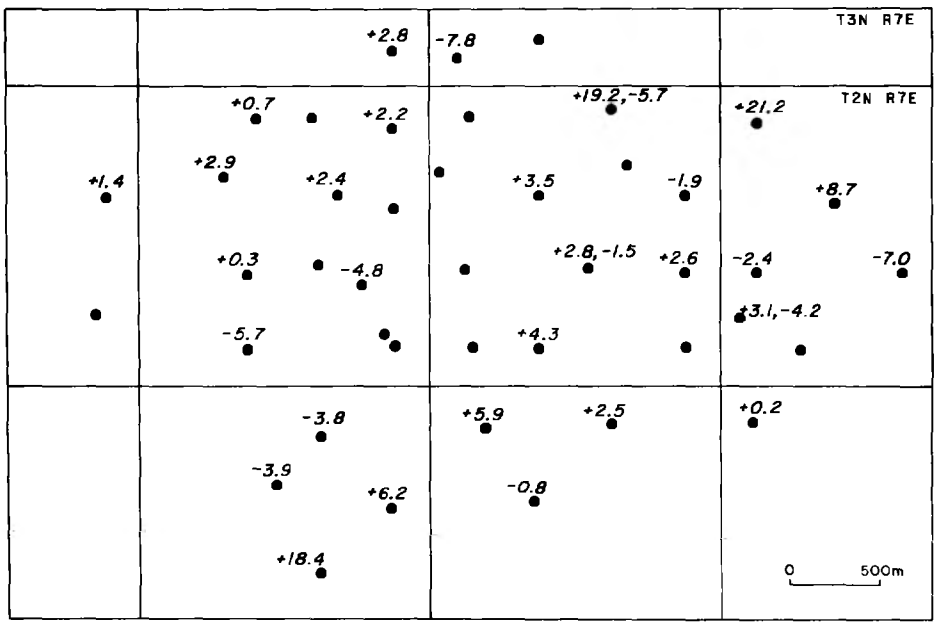

FIG. 6. Temperature residuals (°C) for Pineview wells. The temperature residuals are defined as (corrected BHT) − (estimated temperature), where the estimated temperature is calculated from a forward application of the preferred solution gradients from the l_2 inversion (Table 2).

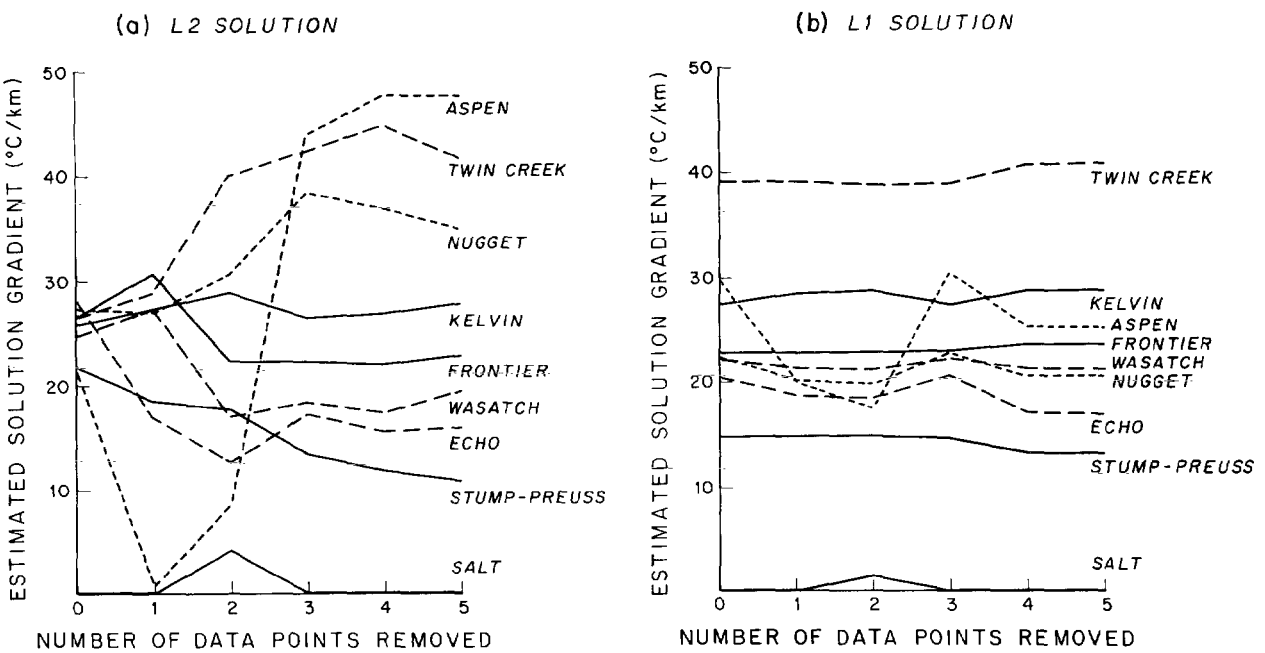

FIG. 7. Formation thermal gradients determined from inversion of BHT data. As the data point representing the highest residual is removed, the stability of the l_2 solution increases. After removal of three BHTs, the solution has stabilized and is similar to the l_1 solution. The preferred solution is chosen as that which occurs after the third point has been removed. The l_1 solution is essentially unaffected by removal of outlying data points, indicating that it is more robust than the l_2 solution.

BHT data contain random error which the inversion has removed.

The estimated temperature field includes first-, second-, and third-order effects. To first order, temperature increases with depth at an average gradient of 24°C/km. A second-order effect is the different gradient in each formation. For example, gradient estimates of 19°C/km and 17°C/km for the Wasatch and Echo Canyon formations, respectively, result in isotherm spacings that are more than twice as wide as the spacing in the high-gradient (43°C/km) Twin Creek limestone. A third-order effect appears implicitly in Figure 8 in the curvature of isotherms. Since heat flow is perpendicular to isotherms, the gentle downward curvature of the isotherms from west to east (left to right) implies that heat is being refracted into the eastern part of the field.

THERMAL CONDUCTIVITY

To estimate heat flow and provide input data for a finite-element thermal model, we made thermal-conductivity measurements on drill cuttings from six of the nine formations in the inversion analysis. Samples were unavailable for the remaining three formations. Measurements were made with a modified divided bar apparatus following the procedure of Sass et al. (1971) in which water-saturated drill cuttings are held in small (about 10 cm^3) disc-shaped holders. This method determines k_m, the thermal conductivity of the matrix, or solid rock component. In order to estimate k_{pr}, the actual in-situ conductivity of a porous rock, the rock porosity ϕ must be known. Furthermore, the matrix conductivity is measured in the laboratory at 20°C and must be corrected for the appropriate in situ temperature. Finally, possible anisotropic effects must be taken into account when interpreting the results of the measurements.

The temperature correction was made by assuming that the matrix conductivity is proportional to the reciprocal of the absolute temperature; thus, $k_{m_T} = k_{m_{20}}[293/(T + 273)]$, where k_{m_T} is the matrix conductivity at temperature T °C and $k_{m_{20}}$ is the matrix conductivity as measured in the laboratory at 20°C. Formation porosities were estimated by using formation-density logs, calibrated by density measurements on the drill cuttings. For the petroleum-saturated Nugget sand-

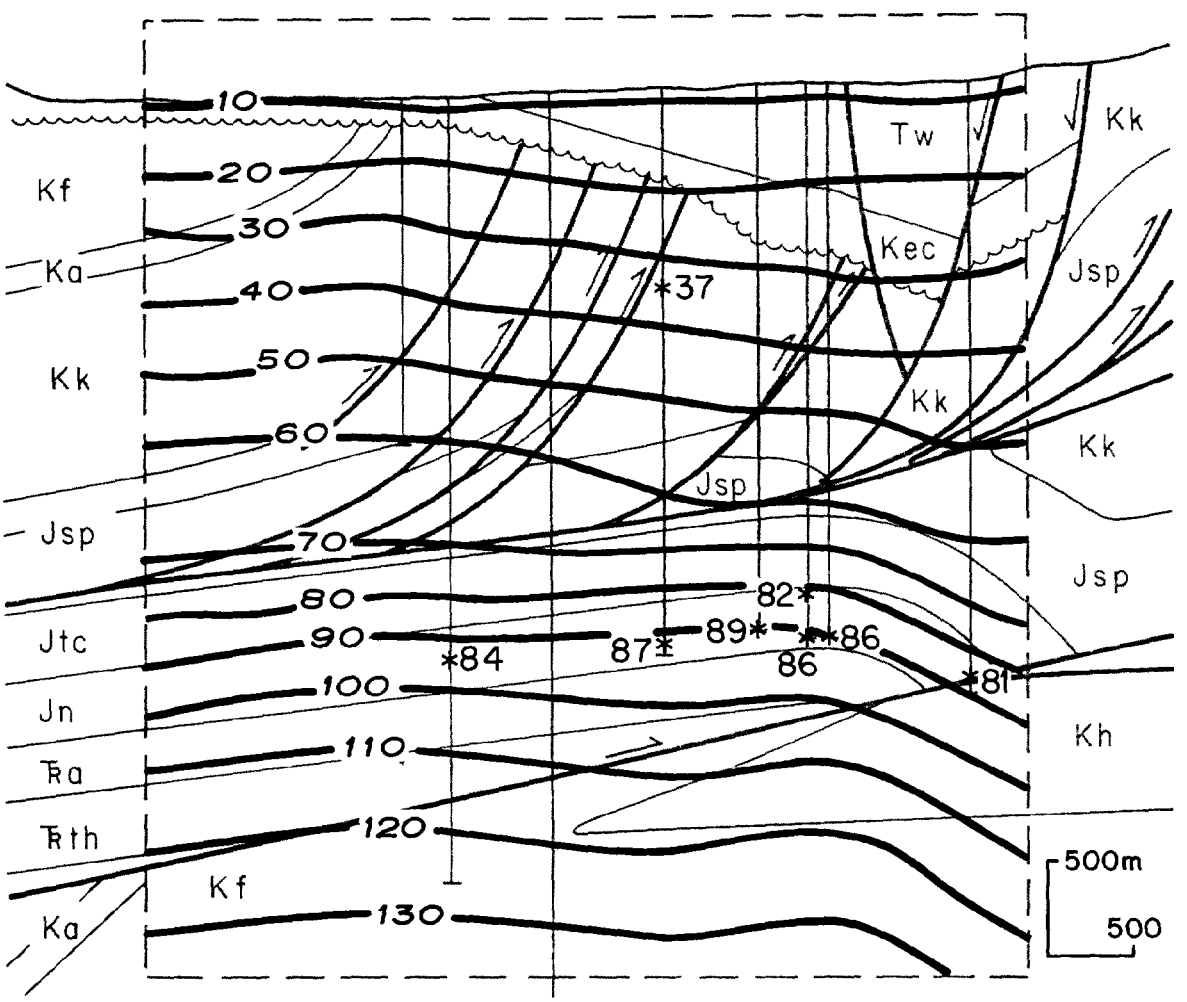

FIG. 8. The temperature field T_{est} at Pineview, estimated using the results of the ℓ_2 inversion gradients. Vertical lines indicate wells from Figure 3. Also shown are the positions (asterisks) and values (°C) of eight corrected BHTs. The temperature field includes first, second, and implicit third-order effects, as discussed in the text.

stone, we used $\phi = 0.12$ as reported by Lelek (1982) for the Nugget in the nearby Anschutz Ranch East field. No corrections for possible anisotropic effects were made; visual inspection of the drill cuttings found an insignificant amount of shale, the only common sedimentary rock known to be highly anisotropic.

The actual porous-rock conductivity k_{pr} was calculated as $k_{pr} = k_w^{\phi} k_{mT}^{(1-\phi)}$, where k_w is the thermal conductivity of water at the in situ temperature T as given by Kappelmeyer and Haenel (1974, p. 223). We assumed that Nugget sandstone was saturated with petroleum and used $k_{oil} = 0.213$ W/m · K (Vacquier, 1984, p. 85). Finally, an effective in situ conductivity $\bar{k}$ for each formation was calculated as a harmonic mean, with each sample weighted by the thickness of the sample interval.

The results of 300 conductivity measurements made on samples from four wells (UPRR 3-2, Newton Sheep 4-10S, Pineview No. 1, and Bingham 2-1A) are shown in Figures 9a, 9b, and 9c. The matrix conductivities ($k_{m_{20}}$) exhibit (almost) the complete range possible for sedimentary rocks, from two values of 0.71 and 0.81 W/m · K for coal samples from the Frontier formation (Pineview No. 1 well) to several values around 7.0 W/m · K for the Echo Canyon quartzite conglomerate (Newton Sheep 4-10S well). The standard deviation of the samples from any one formation reflects primarily the lithological heterogeneity of that formation (Table 2). The Stump-Preuss formation, a uniform fine-grained sandstone, yields a standard deviation of only 0.26 W/m · K for the 41 samples from well UPRR 3-2, while the lithologically diverse Frontier formation, consisting of a series of siltstones, limestones, coal seams, and black shales, has a standard deviation of 0.67 W/m · K for 42 samples. Little lateral variation within formations is observed in thermal-conductivity measurements made on samples from different wells (see Echo Canyon and Stump-Preuss formations in Table 2).

The estimated in situ average formation conductivities for the Pineview field (Table 2) range from 1.89 W/m · K for the Frontier formation to 4.33 W/m · K for the Echo Canyon quartzite conglomerate. The harmonic mean of all six formation conductivities is 2.59 W/m · K. The importance of the temperature and porosity corrections is reflected in the difference between the matrix conductivities and the average in-situ conductivities (Table 2). For example, the Kelvin formation has an mean matrix conductivity of 3.61 W/m · K. However, after the porosity and temperature corrections have been applied, the mean conductivity is 2.74 W/m · K, 24 percent lower.

If the rock porosity ϕ is known, the accuracy of determining the thermal conductivity of a porous rock by this method has been estimated as ± 10 percent by Sass et al. (1971) from a comparison with measurements on core samples. A similar result has been reported by Chapman et al. (1981) and Andrews-Speed et al. (1984), who cite the same 10 percent accuracy level.

SYNTHETIC INVERSIONS AND TEMPERATURE ANOMALIES

The inversion described above is based on an explicit assumption that heat flow is strictly one-dimensional (vertical). Accordingly, it is implicitly assumed that there are no lateral conductivity contrasts and that no heat refraction occurs. However, Pineview is structurally complex, with large lateral changes in lithology (Figure 3). Refraction of heat introduces a systematic model error ε_s into the temperature field that the inversion is largely incapable of resolving.

To assess the effect of heat refraction at Pineview on the inversion results, we designed a two-dimensional (2-D) finite-element model based on Figure 3. The model was used to calculate an exact model temperature field T_{model}, providing data for a series of synthetic inversions. Boundary conditions for the model were chosen as a constant vertical heat flux of 61 mW/m^2 at the base of the mesh, zero heat flux at the lateral boundaries, and fixed temperature at the upper surface. Care was taken to avoid edge effects by extending the grid boundaries well beyond the region of interest. The algorithm was tested against analytic solutions using (1) a homogeneous half-space and (2) a solution for a 2-D cylinder given in Lee and Henyey (1974). The salt was omitted from the model since its representation in the matrix of total thicknesses is very low (1.6 percent) and its occurrence in the Stump-Preuss formation is very irregular. For those formations for which thermal-conductivity measurements were not made, we assigned thermal conductivities of 3.5, 1.5, 2.1, 2.4, 2.4, and 2.0 W/m · K to the Wasatch, Aspen, Ankareh, Thaynes, Woodside-Dinwoody, and Hilliard formations, respectively, as suggested by geologic constraints (Hintze, 1983; Madsen, 1959; Randall, 1952). A uniform conductivity of 2.5 W/m · K was used to extend the grid boundaries.

If heat flow in the model were strictly one-dimensional (vertical), the resulting 1-D temperature field $T_{1\text{-}D}$ could be described or predicted exactly by a thermal-resistance model (Bullard, 1939),

$$T_{1\text{-}D} = T_0 + \sum_j g_j z_j,$$

where the gradient $g_j = (q/k_j)$ is the 1-D gradient in the jth formation, q is the heat flux specified at the base of the finite-element mesh, and k_j is the thermal conductivity of the jth formation. However, because the model structure does not consist of flat-lying layers of constant thermal conductivity, heat flow is not strictly one-dimensional (vertical). Where a horizontal contrast in thermal conductivity is present, heat flows laterally into a more conductive lithology such as the Echo Canyon formation (4.33 W/m · K), away from a resistive lithology such as the Aspen shale (1.50 W/m · K). Thus the model temperature field can be written as

$$T_{model} = T_0 + \sum_j g_j z_j + \varepsilon_s,$$

where ε_s is the perturbation to the 1-D temperature field introduced by 2-D heat refraction. To delineate ε_s, we use a temperature-anomaly map, a contour plot of $(T_{model} - T_{1\text{-}D}) = \varepsilon_s$.

Perturbations to the 1-D temperature field introduced by 2-D refraction are shown in Figure 10. As the surface heat-flow profile (calculated from the finite-element model) above the temperature-anomaly map indicates, heat refracted into the relatively high-conductivity Wasatch (3.50 W/m · K) and Echo Canyon (4.33 W/m · K) formations results in a positive temperature anomaly in the eastern part (right half) of the field. Conversely, a lower than background heat flux results in a negative temperature anomaly in the western part (left half) of the model. The root-mean-square (rms) anomaly over the

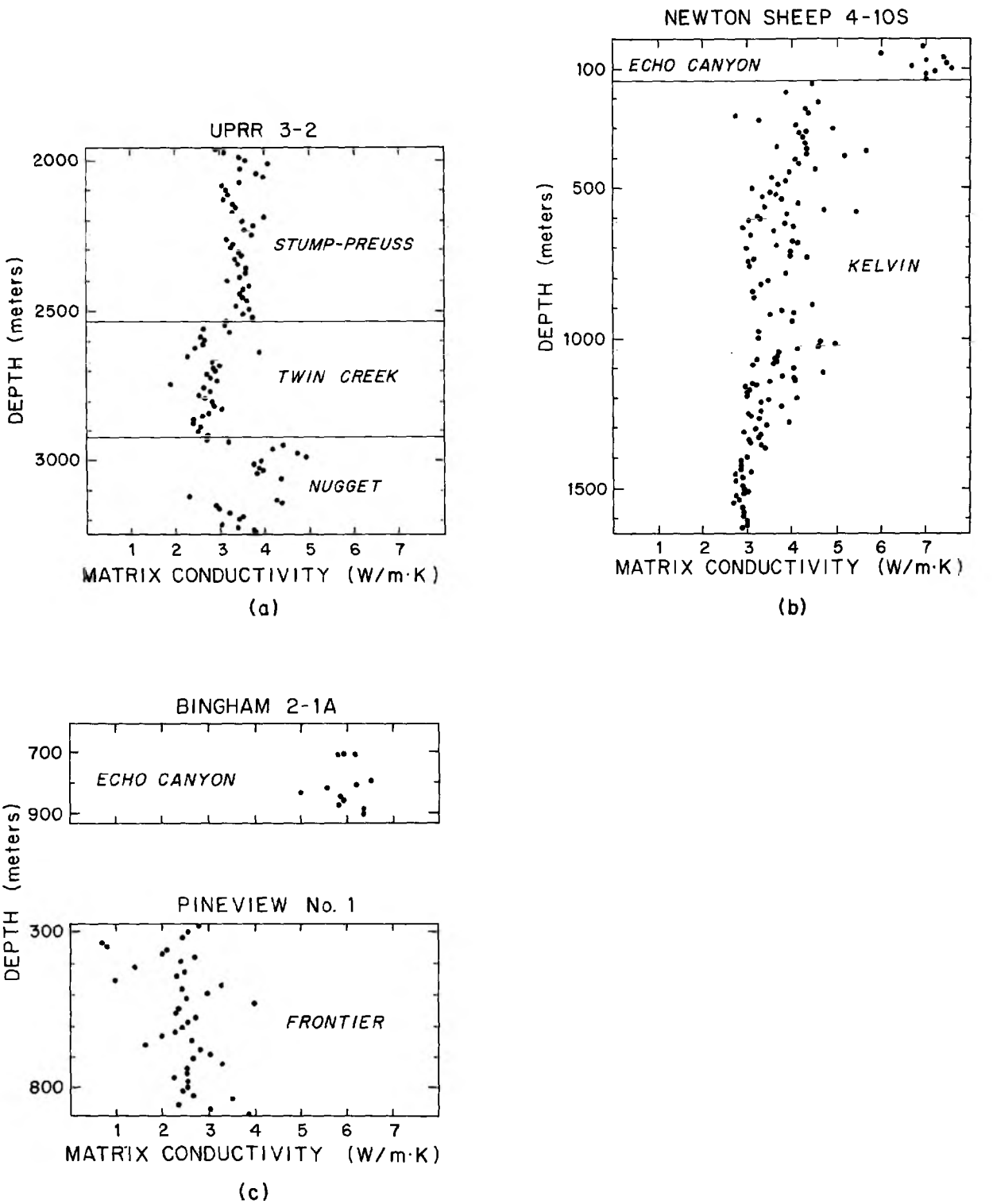

FIG. 9. Matrix thermal-conductivity results as measured in the laboratory at 20°C. Formation boundaries are generally apparent in the thermal-conductivity measurements. To obtain estimates of in situ conductivities, these values must be corrected for porosity and temperature as discussed in the text.

entire area is 2.9°C; the mean anomaly is 1.7°C. The implications of the temperature-anomaly map (Figure 10) are (1) the assumption of 1-D heat transfer upon which the inversion is based is in error, (2) the mean surface heat flow for this cross-section through the Pineview oil field is higher than the background heat flow, and (3) the thermal gradient in each formation is not the 1-D gradient as we have defined it, but some 2-D gradient that varies laterally and vertically across each formation. For example, in the upper part of the section there are large lateral conductivity contrasts, and the gradient in the Echo Canyon formation ranges from 12.1 to 17.2°C/km. On the other hand, in the lower part of the section, the gradient in the laterally homogeneous Twin Creek limestone ranges only from 28.1 to 29.0°C/km.

To assess the effect of heat refraction on the inversion, we inverted the calculated 2-D temperature field T_{model}. To perform such a synthetic inversion, 32 nodal temperatures were selected to represent 32 BHTs in the area of interest. The nodal temperatures were chosen such that the distribution was similar to the actual data set with respect to the formations they penetrated.

Table 3 lists the results of the synthetic inversion, together with both the 1-D gradients and average 2-D gradients computed across the model for each formation. Two features are apparent. First, for the higher-conductivity formations (Echo, Wasatch, Kelvin, Stump-Preuss, Twin Creek, and Nugget), the 2-D gradient is higher than the corresponding 1-D gradient; for the lower-conductivity formations (Frontier and Aspen), the 2-D gradient is lower than its corresponding 1-D counterpart. This simply reflects the refraction of heat into the higher-conductivity formations. Second, the effect of lateral heat refraction appears in the inversion result as a failure to resolve the thermal gradient in the Echo Canyon and Aspen formations. Furthermore, not only does the inversion fail to resolve these gradients, but it gives no evidence of this failure; i.e., the variance does not indicate the departure from the actual 2-D gradients. For example, the estimated standard deviation of the Aspen gradient is 2.0 C/km, but the difference between the 2-D gradient and the inversion estimate is 17.7°C/km. The systematic variation in heat flow across the model (Figure 10) and the resulting perturbation to the temperature field are attributed by the inversion to systematic differences in formation thickness that occur across the model. Lower temperatures in the western part of the field result in a lower estimated gradient in the Aspen shale, because the Aspen shale is present only in the western part of the field. Conversely, higher temperature in the east is attributed largely to a higher gradient in the Echo Canyon formation, since the Echo Canyon formation is considerably thicker in the east than in the west.

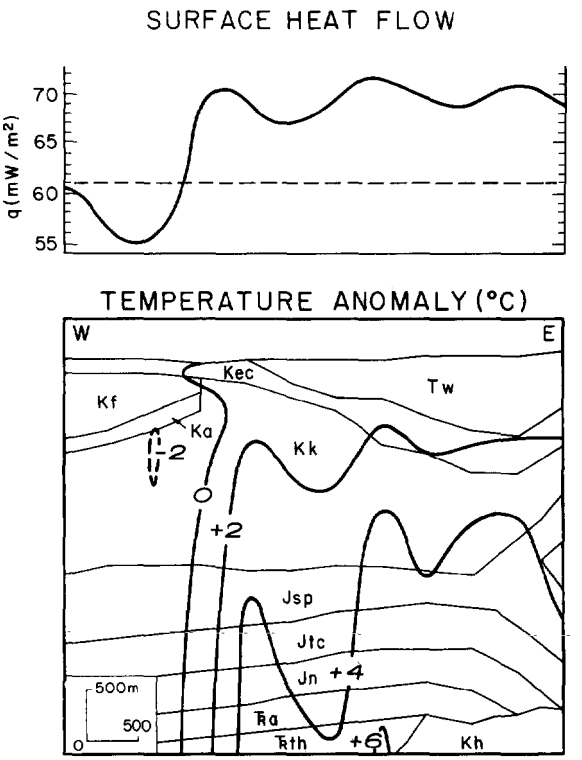

FIG. 10. Temperature-anomaly map. Contours in °C are equal to ε_y, the difference between a 1-D and a 2-D temperature field. Refraction of heat into the right half of the figure is evidenced by the surface heat-flow profile and results in a positive subsurface temperature anomaly. Lower than background heat flow in the left half results in a negative temperature anomaly.

Table 2. Thermal conductivity and porosity data.

Formation	Well	Number of samples	Mean matrix conductivity k_{m20} (W/m · K)	Standard deviation (W/m · K)	Porosity ϕ	In-situ conductivity $\bar{k}$ (W/m · K)
Echo Canyon	Newton Sheep 4-10s	9	6.92	0.49		
Echo Canyon	Bingham 2-1A	12	6.07	0.42		
E.C. average			6.43		.17	4.33
Frontier	Pineview No. 1	42	2.48	0.67	.10	1.89
Kelvin	Newton Sheep 4-10s	128	3.61	0.70	.12	2.74
Stump-Preuss	UPRR 3-2	41	3.50	0.26		
Stump-Preuss	Bingham 2-1A	5	3.20	0.47		
Stump-Preuss	Pineview No. 1	6	3.42	0.28		
S.P. average			3.46		.09	2.65
Twin Creek	UPRR 3-2	33	2.72	0.34	.04	2.16
Nugget	UPRR 3-2	24	3.73	0.66	.12	2.14

To estimate the compound effect of model error ε_s and random error on the gradient estimates, we introduced a random error ε_r into the synthetic BHT data. In keeping with our estimate of error in the corrected BHTs as being on the order of 5 C, we generated a normally distributed random variable with a standard deviation of 5 C and a zero mean, using a method given by Ross (1980, p. 370). The temperature field to be inverted was then $T_{\text{model}} + \varepsilon_r$, where ε_r is the random variable described above. Because the least-squares method has the maximum likelihood of estimating the true solution if the noise is normally distributed with a zero mean, we used only the l_2 method in these inversions.

Inversion was carried out for ten different noise realizations. With the exception of the Kelvin formation, all gradient estimates had significant error and the error was inversely correlated with the total thickness of each formation. The results for the Kelvin and Wasatch formations are shown in Figure 11. For the Kelvin formation, the difference between the estimated gradient (random noise added) and the zero-noise gradient (gradient for no random noise added) is near 2 C/km for most of the trials. More typical is the result for the Wasatch formation in which the behavior is similar, but the magnitude of the error is greater, since the total percent thickness (in the model) of the Wasatch (8 percent) is much less than that of the Kelvin (42 percent).

Although the error in individual formation gradients may be large, the error in a temperature field estimated from the forward application of these synthetic-inversion gradients is smaller than the likely error (5 C) in any single corrected BHT. For each of the ten noise realizations, the inversion gradients were used to estimate or predict the temperature field as

$$T_{\text{predicted}} = T_0 + \sum_j g_{\text{est}_j} z_j,$$

where g_{est_j} is the gradient in the jth formation as estimated by the inversion of the noisy, synthetic (model) temperature data. The error was then calculated as $T_{\text{model}} - T_{\text{predicted}}$; for the ten trials the mean rms error was found to be 2.8 C. A typical result for one of the trials is delineated graphically in Figure 12, a temperature-anomaly map or contour plot of the temperature error as defined above. The map confirms that the largest error is everywhere smaller than 5 C, the probable error in any single corrected BHT.

HEAT FLOW

Unlike the geothermal gradient, which is subject to large local variations, basal heat flow tends to be characteristic of a tectonic province. Therefore, it is the most fundamental quantity which can be used to characterize the thermal state at Pineview.

The average local heat flow at Pineview is 65 mW/m^2, cal-

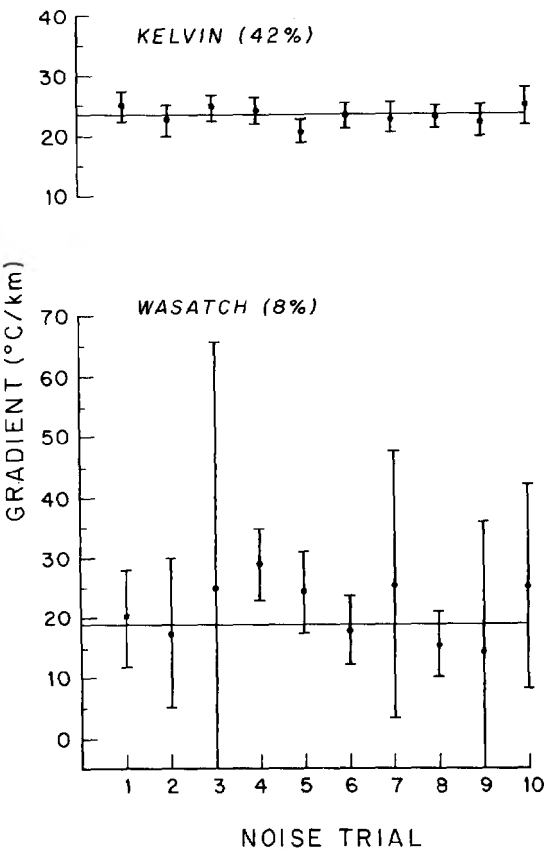

FIG. 11. Thermal gradients (±one standard deviation) for the Kelvin and Wasatch formations. The gradients were calculated by a synthetic inversion of a noisy, 2-D temperature field. Ten different noise trials were done. The solid line is the estimate returned when no random noise was added.

Table 3. Synthetic inversion results.

Formation	Thermal conductivity (W/m · K)	1-D gradient (°C/km)	2-D gradient (°C/km)	Inversion estimate (°C/km)	Error (°C/km)	σ_m (°C/km)
Echo Canyon	4.33	14.1	15.6	19.6	+4.0	0.8
Wasatch	3.50	17.4	19.8	18.8	−1.0	0.4
Kelvin	2.74	22.3	23.5	23.5	0.0	0.1
Stump-Preuss	2.65	23.0	23.7	25.4	+1.7	0.4
Twin Creek	2.16	28.2	28.5	27.4	−1.1	0.5
Nugget	2.14	28.5	28.7	29.6	+0.9	0.6
Frontier	1.89	32.3	30.4	29.1	−1.3	0.4
Aspen	1.50	40.7	37.2	19.5	−17.7	2.0

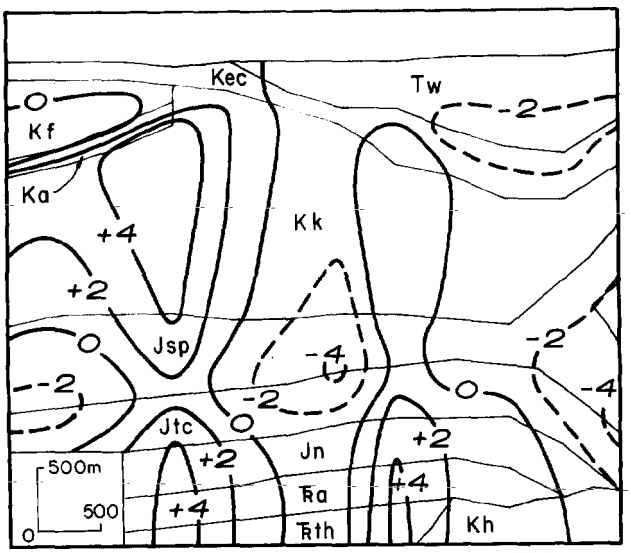

FIG. 12. Temperature-anomaly map. Contours in °C are a measure of the likely error in a temperature field estimated by a forward application of formation thermal gradients obtained from inversion of synthetic data that contain both systematic and random error. The largest error is everywhere smaller than the likely error (±5 C) in any single corrected BHT.

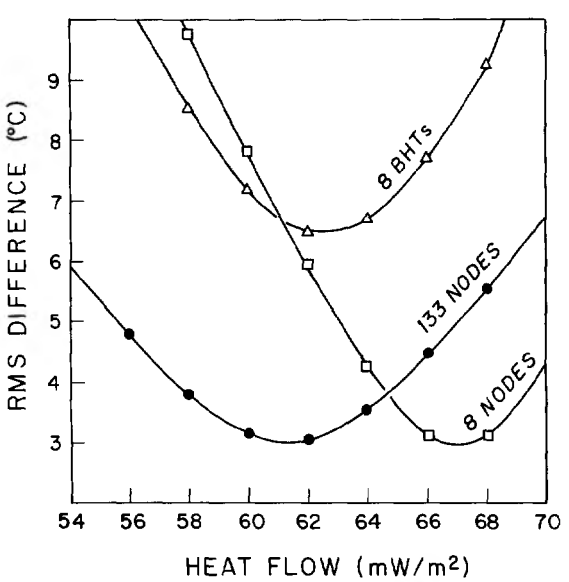

FIG. 13. The rms temperature difference (°C) between the model temperature field and the estimated temperature field T_{est} as calculated at (1) 133 nodes in the finite-element model (circles) and (2) eight nodes corresponding to the locations of the BHTs (squares). Also shown is the rms temperature difference (°C) between the model temperature field and eight corrected BHTs (triangles).

culated as the product of an average gradient (24°C/km) and the harmonic mean of nine formation thermal conductivities. However, modeling results (Figure 10) show that the local heat flow at Pineview is higher than the background heat flow, due to heat refraction into the eastern two-thirds of the field. Therefore, this 1-D estimate of heat flow at Pineview is locally accurate, but higher than the true background heat flow.

In the presence of lateral conductivity variations, an alternative method for estimating the background heat flow must be implemented. Since the BHT inversion returns a best estimate T_{est} of the actual temperature field (Figure 8), a best estimate of the background heat flow is that which reproduces this temperature field in the known thermal-conductivity structure. Proceeding in a similar manner to the synthetic inversions, we varied basal heat flow into the finite-element model and calculated the resultant rms and mean difference between the two temperature fields. The best estimate of the background heat flow is that which results in a minimum difference between the two temperature fields. This is essentially the same method originated by Henry and Pollack (1985) and used by Bauer and Chapman (1986).

The resultant rms difference as a function of heat flow is shown in Figure 13. A minimum rms difference of 3.0°C occurs at $q = 61$ mW/m^2; a zero-mean difference is also found at $q = 61$ mW/m^2. Figure 13 also shows the rms difference between the model temperature field and (1) eight corrected BHTs shown in Figure 8 and (2) T_{est} as calculated at eight nodal points corresponding to the locations of these BHTs. The rms difference between the corrected BHTs and the model temperature field reaches a minimum of 6.5°C at 63 mW/m^2; the rms difference calculated using T_{est} (at eight nodal points) reaches a minimum of 3.0°C at 66 mW/m^2. The model temperature field has no a priori connection with the inversion result; thus, the lower rms difference that results when T_{est} is compared to the model temperature field (as opposed to comparing corrected BHTs) is an independent confirmation that the inversion procedure removes random error from the corrected BHT data. The different minima in all three curves reflect the local variation in heat flow and temperature structure throughout the field depicted in Figure 10.

We estimate the uncertainty in local heat flow (65 mW/m^2) by assuming Gaussian statistics and uncorrelated errors. Random error in individual corrected BHTs is estimated as 5 C; surface-temperature estimations and the Horner correction itself are considered to have systematic errors of 2.5°C. This leads to a 6 percent error in the average gradient.

For each formation matrix conductivity we consider the 10 percent error inherent in the measuring method itself and a likely error of 25 percent in the formation porosities. For formations which were not measured, we assume uncertainties of 30 percent. Propagation of the above error sources yields a probable error of 6 percent in the harmonic-mean conductivity of all formations. To this figure, 5 percent is added because of the uncertainty involved in the temperature correction made to matrix conductivities (see data in Roy et al., 1981). Propagation of the gradient error (6 percent) with the conductivity error (11 percent) yields a likely heat-flow error of 13 percent. Interpreting the result of the finite-element modeling as a correction to the local heat-flow estimate, the best estimate of the background heat flow at Pineview is 61 mW/m^2 (±13 percent).

DISCUSSION

Determination of thermal conductivity is often a limiting factor in heat-flow estimates; the uncertainty involved with high-precision logging of equilibrium temperatures in-situ introduces a negligible error into a heat-flow estimate. Our results suggest that heat-flow estimates with a reasonable accuracy can be made by treating a BHT data set in a statistical manner that removes most of the random error. Furthermore, the inversion of a BHT data set has advantages over the conventional methodology of high-precision temperature logging in shallow drillholes. Most BHTs are measured at depths sufficient (greater than 500 m) to be immune to the influence of near-surface factors (see Blackwell et al., 1980 and Bauer and Chapman, 1986, for examples of problems inherent in making heat-flow estimates from temperatures measured in shallow drillholes). Additionally, in structurally complex areas, the likelihood of lateral heat refraction implies that any single temperature log has a probability of being biased; inversion of a BHT data set samples the entire area.

Synthetic modeling is crucial to the interpretation of inversion results and thus is an integral part of the Pineview analysis, as it was for the inversion of BHT data from the Michigan Basin by Speece et al. (1985). However, there are differences in our approaches. The Michigan Basin modeling was largely confined to testing the stability of the inversion gradients. Stability is defined by Speece et al. (1985, p. 1324) as a measure of the resistance of the solution to changes in the data. That is, if relatively small changes in the data lead to large changes in the solution, then the solution cannot be valid, since the data vector is known to contain error. However, although stability is a necessary criterion for a valid solution, it is not a *sufficient* criterion. A solution may be stable but still bear no resemblance to the true solution. Therefore, we chose to perform a series of synthetic inversions that assessed the limitations of the inversion analysis in a more stringent sense. This series included a comparison of true model gradients and inversion estimates (Figure 11), and, more importantly, a comparison of temperature fields predicted or estimated from inversion results and a true (model) temperature field (Figure 12). The results show that the inversion is sensitive to the actual temperature change across any formation rather than to the formation gradient. Thus, the resolution of formation gradients is relatively poor (Figure 11); but the temperature field, as reconstructed from the forward application of these same poorly resolved gradients, has excellent resolution in the sense that the probable error anywhere is less than the probable error in any single corrected BHT. However, it must be noted that this error, as shown by the temperature-anomaly map (Figure 12), results from the optimal application of a least-squares method to a data set that has (1) a zero mean error and (2) a normal distribution. Real (as opposed to synthetic) data sets do not adhere strictly to either of these constraints; in practice the ability to estimate basin temperatures through inversion of BHT data is determined largely by the mean error in the BHT correction used.

ACKNOWLEDGMENTS

Acknowledgment is made to the donors of the Petroleum Research Fund, administered by the ACS, for partial support of this research. Partial support was also received from Chevron Oil Field Research Company and Tenneco Oil Company. We thank G. Schuster for making computational facilities available. J. Dent of the Utah Geological and Mineralogical Survey made the drill chip samples available for thermal-conductivity measurements. The research presented profited from the collective efforts of our colleagues: B. Powell suggested the ℓ_1 inversion; S. Willett wrote the finite-element program and assisted in the model design; F. Brigaud assisted in porosity calculations and helped digitize the well logs. This paper was completed while DSC was at the Pacific Geoscience Center; it constitutes contribution no. 11487 of the Geological Survey of Canada.

REFERENCES

American Association of Petroleum Geologists (AAPG), 1976, Basic data file from AAPG geothermal survey of North America: Univ. of Oklahoma.

Andrews-Speed, C. P., Oxburgh, E. R., and Cooper, B. A., 1984, Temperatures and depth-dependent heat flow in Western North Sea: Bull., Am. Assn. Petr. Geol., **68,** 1764–1791.

Bauer, M. S., and Chapman, D. S., 1986, Thermal regime at the Upper Stillwater dam site, Uinta Mountains, Utah: implications for terrain, microclimate and structural corrections in heat flow studies: Tectonophys., **128,** 1–20.

Blackwell, D. D., Steele, J. L., and Brott, C. A., 1980, The terrain effect on terrestrial heat flow: J. Geophys. Res., **85,** 4757–4772.

Bullard, E. C., 1939, Heat flow in South Africa: Proc. Roy. Soc. London, Series A, **173,** 474–502.

Chapman, D. S., Clement, M. D., and Mase, C. W., 1981, Thermal regime of the Escalante Desert, Utah, with an analysis of the Newcastle geothermal system: J. Geophys. Res., **86,** 11735–11746.

Chapman, D. S., Keho, T. H., Bauer, M. S., and Picard, M. D., 1984, Heat flow in the Uinta Basin determined from bottom hole temperature (BHT) data: Geophysics, **49,** 453–466.

Edman, J. D., and Surdam, R. C., 1984, Influence of overthrusting on maturation of hydrocarbons in Phosphoria formation, Wyoming-Idaho-Utah overthrust belt: Bull., Am. Assn. Petr. Geol., **68,** 1803–1817.

Henry, S. G., and Pollack, H. N., 1985, Heat flow in the presence of topography: Numerical analysis of data ensembles: Geophysics, **50,** 1335–1341.

Hintze, L. F., 1983, Geologic history of Utah: Brigham Young Univ. Press.

Jam, P. L., Dickey, P. A., and Tryggvason, E., 1969, Subsurface temperature in south Louisiana: Bull., Am. Assn. Petr. Geol., **53,** 2141–2149.

Kappelmeyer, O., and Haenel, R., 1974, Geothermics with special reference to application: Gebrüder-Borntraeger.

Lamerson, P. R., 1982, The Fossil Basin and its relationship to the Absaroka thrust system, Wyoming and Utah, *in* Powers, R. B., Ed., Geologic studies of the Cordilleran thrust belt: Rocky Mountain Assn. Geol., 279–340.

Lawson, C. L., and Hansen, R. J., 1974, Solving least squares problems: Prentice-Hall, Inc.

Leadholm, R. H., Ho, T. T. Y., and Sahai, S. K., 1985, Heat flow, geothermal gradients and maturation modelling on the Norwegian continental shelf using computer methods, *in* Thomas, B. M., Ed., Petroleum geochemistry in exploration of the Norwegian shelf: Graham and Trotman.

Lee, T. C., and Henyey, T. L., 1974, Heat-flow refraction across dissimilar media: Geophys. J. Roy. Astr. Soc., **39,** 319–333.

Lelek, J. J., 1982, Anschutz Ranch East Field, northeast Utah and southwest Wyoming, *in* Powers, R. B., Ed., Geologic studies of the Cordilleran thrust belt: Rocky Mountain Assn. Geol., 619–631.

Luheshi, M. N., 1983, Estimation of formation temperatures from borehole measurements: Geophys. J. Roy. Astr. Soc., **74,** 747–776.

Madsen, J. H., 1959, Geology of the Lost Creek-Echo Canyon area, Morgan and Summit counties, Utah: M.S. Thesis, Univ. of Utah.

Majorowicz, J. A., and Jessop, A. M., 1981, Regional heat flow patterns in the western Canadian Sedimentary Basin: Tectonophys., **74,** 209–238.

Menke, W., 1984, Geophysical data analysis: discrete inverse theory: Academic Press Inc.

Randall, A. G., 1952, Areal geology of the Pinecliff area, Summit County, Utah: M.S. thesis, Univ. of Utah.

Reiter, M., Eggleston, R. E., Broadwell, B. R., and Minier, J., 1986, Estimates of terrestrial heat flow from petroleum tests along the

Rio Grande Rift in central and southern New Mexico: J. Geophys. Res., **91,** 6225–6245.
Reiter, M., Mansure, A. J., and Shearer, C., 1979, Geothermal characteristics of the Colorado Plateau: Tectonophys., **61,** 183–195.
Ross, S., 1980, A first course in probability: Macmillan Publ. Co.
Roy, R. F., Beck, A. E., and Touloukian, Y. S., 1981, Thermophysical properties of rocks, *in* Touloukian, Y. S., and Ho, C. Y., Eds., Physical properties of rocks and minerals: McGraw-Hill Book Co.
Sass, J. H., Lachenbruch, A. H., and Munroe, R. J., 1971, Thermal conductivity of rocks from measurements on fragments and its application to heat-flow determinations: J. Geophys. Res., **76,** 3391–3401.
Sass, J. H., Lachenbruch, A. H., Munroe, R. J., Greene, G. W., and Moses, T. H., Jr., 1971, Heat flow in the western United States: J. Geophys. Res., **76,** 6376–6413.
Speece, M. A., Bowen, T. D., Folcik, J. L., and Pollack, H. N., 1985, Analysis of temperatures in sedimentary basins: the Michigan Basin: Geophysics, **50,** 1318–1334.
Vacquier, V., 1984, Oil fields—a source of heat flow data: Tectonophys., **103,** 81–98.
Waples, D. W., 1980, Time and temperature in petroleum formation: application of Lopatin's method to petroleum exploration: Bull., Am. Assn. Petr. Geol., **64,** 916–926.
Warner, M. A., 1982, Source and time of generation of hydrocarbons in the Fossil basin, western Wyoming thrust belt, *in* Powers, R. B., Ed., Geologic studies of the Cordilleran thrust belt: Rocky Mountain Assn. Geol., 805–815.
Willett, S. D., and Chapman, D. S., 1987, Analysis and interpretation of temperatures and thermal processes in the Uinta Basin: Bull., Can. Soc. Petr. Geol., in press.